Growing Length Scales and Their Relation to Timescales in Glass-Forming Liquids

Smarajit Karmakar,[1] Chandan Dasgupta,[2] and Srikanth Sastry[1,3]

[1]TIFR Centre for Interdisciplinary Sciences, Narsingi, Hyderabad 500075, India

[2]Centre for Condensed Matter Theory, Department of Physics, Indian Institute of Science, Bangalore 560012, India; email: cdgupta@physics.iisc.ernet.in

[3]Theoretical Sciences Unit, Jawaharlal Nehru Centre for Advanced Scientific Research, Jakkur Campus, Bangalore 560064, India

Annu. Rev. Condens. Matter Phys. 2014. 5:255–84

First published online as a Review in Advance on January 13, 2014

The *Annual Review of Condensed Matter Physics* is online at conmatphys.annualreviews.org

This article's doi:
10.1146/annurev-conmatphys-031113-133848

Keywords

glass transition, dynamic length scale, static length scale, dynamic heterogeneity, four-point susceptibility, configurational entropy, random first-order transition theory, point-to-set length scale

Abstract

The question of whether the dramatic slowing down of the dynamics of glass-forming liquids near the structural glass transition is caused by the growth of one or more correlation lengths has received much attention in recent years. Several proposals have been made for both static and dynamic length scales that may be responsible for the growth of timescales as the glass transition is approached. These proposals are critically examined with emphasis on the dynamic length scale associated with spatial heterogeneity of local dynamics and the static point-to-set or mosaic length scale of the random first-order transition theory of equilibrium glass transition. Available results for these length scales, obtained mostly from simulations, are summarized, and the relation of the growth of timescales near the glass transition with the growth of these length scales is examined. Some of the outstanding questions about length scales in glass-forming liquids are discussed, and studies in which these questions may be addressed are suggested.

1. INTRODUCTION

The behavior of glass-forming liquids as they are cooled or compressed toward the glass transition is one of the most extensively studied but poorly understood problems in classical condensed matter physics (1, 2). The most prominent feature of this behavior is a dramatic slowing down of the dynamics. This is manifested in the temperature dependence of the shear viscosity η, the diffusion coefficient D, and the structural relaxation time τ as well as other measures of the slowness of the dynamics. The slowing down of the dynamics in so-called fragile (3) liquids is well described by the super-Arrhenius Vogel-Fulcher-Tammann (VFT) form (4–6)

$$X(T) \propto \exp\left[C_x T_0/(T - T_0)\right], \qquad 1.$$

where X represents η, D^{-1}, or τ, and the fragility parameter C_x depends on the quantity being considered. This form predicts a divergence of timescales at a nonzero temperature T_0, which typically turns out to be approximately 10% lower than the glass transition temperature T_g, defined conventionally as the temperature at which the viscosity reaches the value of 10^{12} Pa.s. Because the liquid cannot be equilibrated (even in a restricted sense, excluding the regions of phase space near the crystalline state, which is believed to be the true equilibrium state at low temperatures) in experimentally achievable timescales at temperatures lower than T_g, the validity of the VFT form, and hence of the conclusion that timescales would diverge at the VFT temperature T_0 if the liquid could be equilibrated at temperatures all the way down to T_0, rests on fitting the data at temperatures higher than T_g to the VFT form and extrapolation of this fit to lower temperatures. Thus, the occurrence of a finite-temperature divergence of timescales in glass-forming liquids cannot be established conclusively from experimental observations. Other functional forms, which predict a divergence of timescales only at $T = 0$ or indicate a different form of divergence at a nonzero temperature, have been proposed in the literature (7), but the VFT form continues to be the most popular one among researchers in this field.

Another interesting observation that relates the dynamics of glass-forming liquids to their equilibrium properties is the so-called Kauzmann paradox (8), which involves the excess entropy $S_{ex}(T)$, defined as the difference between the entropy of the supercooled liquid and that of the equilibrium crystalline solid at the same temperature T. For a large number of glass-forming liquids, $S_{ex}(T)$ is found to extrapolate to zero at a temperature T_K (called the Kauzmann temperature) that turns out to be close to the VFT temperature T_0. This observation suggests a close connection between the growth (and possible divergence) of timescales and the vanishing of the excess entropy, quantitatively expressed by the Adam-Gibbs relation (9) between the viscosity and the excess entropy:

$$\eta(T) \propto \exp\left[C/\left(TS_{ex}(T)\right)\right], \qquad 2.$$

where C may be thought to be related to a high-temperature-activation free energy. This relation, proposed by Adam & Gibbs many years ago from heuristic arguments, is found to be satisfied in experiments and simulations on a wide variety of glass-forming liquids (10 and references therein). The validity of this relation suggests that the dramatic growth of relaxation times is a consequence of a thermodynamic, entropy-vanishing transition that would take place at $T = T_0 = T_K$ if equilibrium could be maintained down to this temperature. Another interesting and universal feature of glassy dynamics is the nonexponential, multistep decay of time-dependent density correlation functions, with well-defined short-time (β) and long-time (α) regimes. The structural relaxation time τ considered above refers to the long-time α-relaxation process.

The experimental features summarized above strongly suggest the occurrence of cooperative processes in glass-forming liquids, which, in turn, implies the presence of growing length scales that describe the spatial extent of correlated or cooperatively rearranging regions, a term first used by Adam & Gibbs (9) in their heuristic description of glassy dynamics. The expectation that the growth of relaxation times should be related to a growing length scale arises partly from an analogy with critical phenomena in which the divergence of a correlation length, defined from the spatial decay of the equal-time correlation of the appropriate order-parameter field, at a continuous phase transition leads to a divergence of the relaxation time (11). The critical slowing down at continuous phase transitions usually obeys conventional dynamic scaling in which the relaxation time τ grows as a power of the correlation length ξ, which diverges at the transition point

$$\tau \propto \xi^z, \qquad 3.$$

where z is the so-called dynamic critical exponent. The growth of the relaxation time near the phase transition in certain disordered systems, such as the random-field Ising model (12), is believed to follow a different form known as activated dynamic scaling:

$$\tau \propto \exp(A\xi^z/T), \qquad 4.$$

where A is a constant. The similarity of this scaling behavior with the VFT form of Equation 1, where $\xi \propto (T - T_0)^{-1/z}$, and with the Adam-Gibbs form of Equation 2, with $\xi \propto S_{ex}^{-1/z}$, has prompted the development of theories of the glass transition in which the vanishing of the excess entropy coincides with the divergence of a suitably defined length scale, and this divergence of the length scale leads to a divergence of timescales. More recently, it has been shown (13) that under fairly general conditions, a divergence of τ at a nonzero temperature and finite pressure must be accompanied by the divergence of a suitably defined length scale.

Although the arguments for the existence of one or more growing length scales in glass-forming liquids are quite compelling, it is by no means obvious how such length scales should be defined and measured. The glass transition is not accompanied by any obvious change in structure because the structure of the glassy state is quite similar to that of the liquid above the glass transition. It is not clear whether the interesting features of glassy dynamics mentioned above arise from an underlying phase transition, and there is no consensus on what order parameter should be used to describe such a transition or whether it even exists. Therefore, the usual method of extracting correlation lengths from appropriate correlation functions and related susceptibilities does not lead to a unique prescription for defining length scales relevant to the glass transition. As a result, a wide variety of proposals have been made in recent years for defining length scales that may be appropriate for describing glassy dynamics. The objective of this article is to provide a critical review of these proposals and to discuss the extent to which these proposals improve our understanding of the results of experiments and simulations on glass-forming liquids. The basic questions addressed here are as follows:

1. Are the proposed length scales universal in the sense that they can be used to describe the behavior of a wide variety of glass-forming liquids? How do they grow as temperature decreases?
2. Are the different length scales proposed in the literature related to one another?
3. What is the relation (if any) between static and dynamic length scales?
4. Is any one of the proposed length scales causally related to the dramatic growth of timescales near the glass transition?

Because most of the proposed length scales are derived from quantities that cannot be easily measured in experiments, one has to rely mostly on simulations of model liquids in the quest

for answers to these questions. For this reason, in this review we concentrate on the behavior of atomistic glass-forming liquids with simple interactions that can be simulated using standard methods and equilibrated (in the restricted sense mentioned above) at temperatures and densities for which some of the defining features of glassy dynamics mentioned above are observed. We also examine possible connections between dynamic and equilibrium properties of these systems. There exists a class of lattice-gas models with kinetic constraints (14) that exhibit interesting dynamic behavior, such as rapid growth (and divergence in some cases) of timescales and associated dynamical length scales, but trivial equilibrium behavior. We do not consider these models here because a clear connection of these models with simple liquids of interacting particles has not been established, although several interesting attempts have recently been made (e.g., see 15). We also do not consider the athermal process of jamming (16), which exhibits certain similarities with the glass transition. Length scales that emerge in studying mechanical behavior of amorphous solids (17) are also not addressed in a systematic way in this review. Interested readers are referred to existing review articles on these topics (14, 16, 17).

This review is organized as follows. In Section 2, we describe different existing proposals for growing length scales, with emphasis on the length scale associated with spatial heterogeneity of the local dynamics and the mosaic length scale of the random first-order transition (RFOT) theory (18) of equilibrium glass transition. Section 3 contains a summary of existing results (mostly numerical; experimental in a few cases) for these length scales. The important issue of the relation of growing timescales to these length scales is discussed in Section 4, and we conclude in Section 5 with discussion on the present state of affairs, outstanding questions, and suggestions for future work.

2. PROPOSALS FOR GROWING LENGTH SCALES

The proposals for growing length scales can be broadly classified into two categories: (*a*) dynamical length scales extracted from finite-time behavior of time-dependent correlation functions and associated susceptibilities and (*b*) static length scales derived from equilibrium averages (in the restricted sense mentioned above). We start this section with a description of a dynamic length scale associated with spatial heterogeneity of the local dynamics. This is followed by descriptions of various proposals for static length scales, with emphasis on the mosaic or point-to-set length scale.

2.1. Length Scale of Dynamic Heterogeneity

In studies of glassy dynamics, the term dynamic heterogeneity (DH) is used to describe the spatially heterogeneous nature of the local dynamics. A variety of experimental (19, 20) and numerical (21) studies have established the occurrence of DH in liquids near the glass transition. The simplest way of describing DH is to consider the distribution of the magnitudes of the displacements of the particle in a liquid over some time interval. It has been found that at intermediate times, the distribution of displacements in liquids becomes non-Gaussian, with the development of large tails (22) at low temperatures. The non-Gaussian parameter α_2, which quantifies the deviation of the distribution from the Gaussian behavior expected in simple diffusion, is defined as

$$\alpha_2(t) = \frac{2\langle r^4(t)\rangle}{5\langle r^2(t)\rangle^2} - 1, \qquad 5.$$

where $r(t)$ is the magnitude of the displacement of a particle in time t. This parameter exhibits a pronounced peak at a characteristic time t^*. Using the value of α_2 as a measure, the degree of

heterogeneity is maximum at t^*, and some of the early analyses of dynamical heterogeneity focused on behavior at time $t = t^*$. In this time window, the actual distribution can be compared to the expectation for the given mean-squared displacement if the function is Gaussian. Such a comparison, shown in the left panel of **Figure 1**, indicates that a fraction of the particles move by a larger distance than expected. Defining a cutoff r^*, where the Gaussian reference and the actual van Hove function intersect, particles that have moved by distances larger than r^* are identified as mobile or fast particles. These were found to be typically about 5% of the total population (23).

A very important observation is that particles with similar mobility tend to form clusters, indicating that the local mobilities are spatially correlated. An example of such clusters is provided in the right panel of **Figure 1**, which shows experimental results for the spatial distribution of fast particles in a colloidal fluid near the glass transition (24). The presence of two well-defined clusters can be clearly seen in this figure. These clusters have finite lifetimes. Detailed simulations (25) have shown that the clusters of cooperatively moving mobile particles have a string-like structure, whereas clusters of mobile and immobile particles are more compact. These observations have led to the development of the excitation chain theory of the glass transition (26). Starr et al. (27) analyzed the geometry of string-like clusters and clusters of mobile and immobile particles, significantly extending results available from earlier work (25, 28). Mobile and immobile particle clusters have fractal dimensions in the range of 2–2.5, comparable to lattice animals and branched polymers with screened excluded volume interactions, whereas strings have fractal dimensions in the range of 5/3–2, i.e., spanned by the fractal dimension of self-avoiding random walks and of simple random walks.

It is clear from these results that DH has one (or more) length scale(s) that characterize the spatial correlations of local mobility. Roughly speaking, these length scales correspond to the typical sizes of the clusters mentioned above. In practice, however, it is difficult to extract quantitative estimates of the length scale(s) of DH from studies of these clusters (27). These difficulties arise from ambiguity in the definition of slow and fast particles, noncompact geometry of the clusters, etc. Most quantitative studies of the length scale of DH have therefore been based on

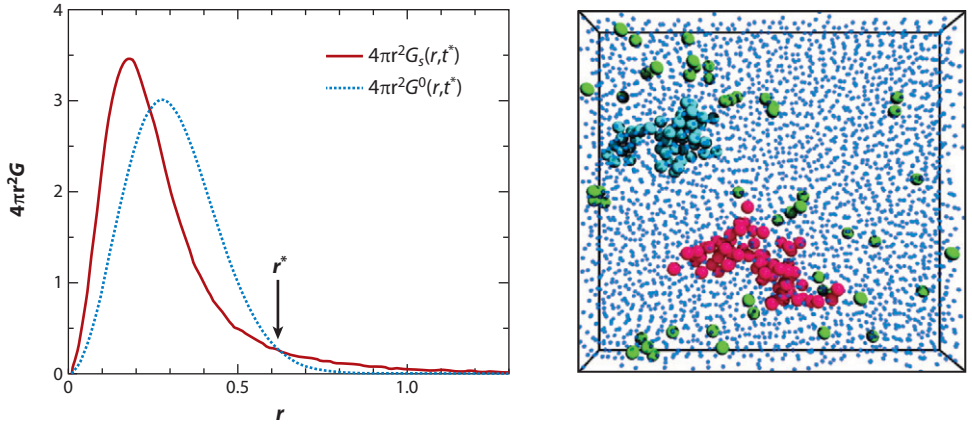

Figure 1

(*a*) Illustration of how the displacement cutoff r^* is determined. $G_s(r, t)$ is the self part of the van Hove correlation function, and $G^0(r, t)$ is the Gaussian approximation with the same mean-square displacement. Particles that have moved more than r^* are considered to be mobile. Adapted from Reference 25. (*b*) Clusters formed by "fast" particles in a colloidal fluid near the glass transition. Two large clusters are shown in red (69 particles) and light blue (50 particles). Adapted from Reference 24.

multipoint correlation functions and associated susceptibilities defined from an analogy with corresponding quantities in spin glasses (12). A four-point correlation function introduced in Reference 29 has played a prominent role in these studies. This function is defined as

$$g_4(\mathbf{r},t) = \langle \delta\rho(0,0)\delta\rho(0,t)\delta\rho(\mathbf{r},0)\delta\rho(\mathbf{r},t)\rangle - \langle \delta\rho(0,0)\delta\rho(0,t)\rangle\langle \delta\rho(\mathbf{r},0)\delta\rho(\mathbf{r},t)\rangle, \quad 6.$$

where $\delta\rho(\mathbf{r}, t)$ represents the deviation of the local density at point $\mathbf{r}$ at time t from its average value, and $\langle \ldots \rangle$ represents a thermal or initial time average. This function quantifies the correlation of the relaxation of density fluctuations at two points separated by distance r. A four-point susceptibility may be defined as the $k \to 0$ value of the Fourier transform $g_4(\mathbf{k}, t)$ of this function (30, 31). A variant of this four-point function has been used extensively in numerical studies of DH because it is easier to compute (32). This quantity is obtained from the overlap function $Q(t)$ defined as the average of

$$\tilde{Q}(t) = \sum_{i=1}^{N} w\left(\left|\mathbf{r}_i(0) - \mathbf{r}_i(t)\right|\right), \quad 7.$$

where $\mathbf{r}_i(t)$ is the position of particle i at time t, N is the total number of particles, $w(r) = 1$ if $r \leq a_0$ and zero otherwise, and a_0 is a short-distance cutoff chosen to be close to the distance at which the root-mean-square displacement of the particles as a function of time exhibits a plateau [the precise choice of the form of the window function $w(r)$ or of the cutoff a_0 turns out to be qualitatively unimportant, but the dependence on the choice has been analyzed in some detail in References 33 and 34]. This function may be viewed as the self part of the density correlation function $C(t)$, which is the average of

$$\tilde{C}(t) = \int d\mathbf{r}\rho(\mathbf{r},0)\rho(\mathbf{r},t) \quad 8.$$

over initial times, with the window function $w(r)$ used to treat particle positions separated by distances smaller than a_0, arising from small-amplitude vibrational motion in the cage formed by neighboring particles, as indistinguishable. The fluctuations in this two-point function yield the dynamical four-point susceptibility:

$$\chi_4(t) = \frac{1}{N}\left[\left\langle \tilde{Q}^2(t)\right\rangle - \left\langle \tilde{Q}(t)\right\rangle^2\right]. \quad 9.$$

A closely related four-point susceptibility, defined as the fluctuation of the self part of the intermediate scattering function $F_s(k, t)$, where k is typically the value at the peak of the static structure factor, has also been used in numerical studies of DH (35–37). The self part of the intermediate scattering function is defined as the average of

$$\tilde{F}_s(\mathbf{k},t) = \sum_{i=1}^{N} \exp\left[\mathbf{k}\cdot\left(\mathbf{r}_i(t) - \mathbf{r}_i(0)\right)\right], \quad 10.$$

over initial times.

The typical behavior of $\chi_4(t)$ for a mixture of Lennard-Jones particles (38) is shown in **Figure 2**. The four-point susceptibility reaches a maximum at time τ_4, which is proportional to the structural relaxation time τ, and the peak value of χ_4 increases with decreasing temperature. This behavior

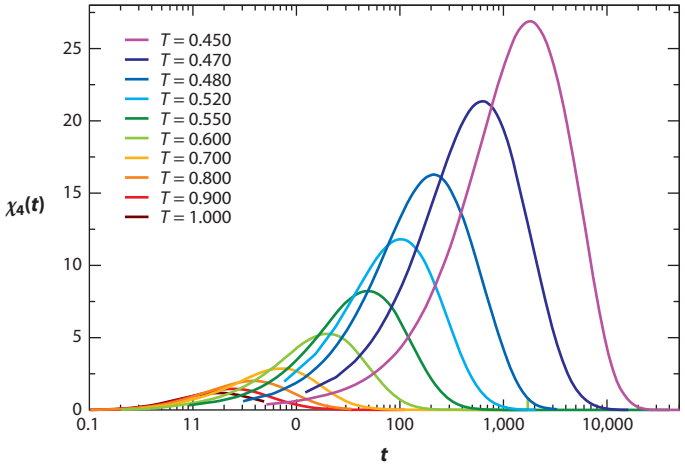

Figure 2

The four-point susceptibility, $\chi_4(t)$, of a three-dimensional binary Lennard-Jones liquid as a function of time t for different temperatures (T). The temperatures are given in reduced units. Adapted from Reference 38.

implies that DH is transient in time, reaching a maximum that is at times comparable to τ, and both the magnitude and the lifetime of DH increase as the glass transition is approached. The growth of the peak value of $\chi_4(t)$, $\chi_4^p \equiv \chi_4(\tau_4)$, is analogous to the growth of the order-parameter susceptibility as a continuous phase transition is approached, indicating the presence of a growing correlation length. There is, however, an important difference: The length scale associated with the growth of χ_4^p must be classified as a dynamical length scale because it describes finite-time behavior.

A variety of analytic results for χ_4 and a related three-point susceptibility have been obtained from inhomogeneous mode coupling theory (MCT) (39, 40), a generalization of the well-known MCT of glassy dynamics (41, 42) in spatially heterogeneous systems. In MCT, an approximate treatment of nonlinearities in the equations for the dynamics of liquids leads to the prediction of a structural arrest with a power-law divergence of the viscosity at an ideal glass transition temperature, T_c. The predictions of MCT provide a fairly accurate account of the results of experiments and simulations in the temperature range that covers the first few decades of the growth of the viscosity. However, the value of T_c obtained from fits of higher-temperature data to a power-law form turns out to be substantially higher than T_g, indicating a breakdown of MCT and a possible crossover in the dynamics. Inhomogeneous MCT predicts power-law divergences of the four-point susceptibility χ_4^p and an associated dynamical correlation length, ξ_d, at temperature T_c:

$$\chi_4^p(T) \propto \left(\frac{T - T_c}{T_c}\right)^{-\gamma}, \; \xi_d(T) \propto \left(\frac{T - T_c}{T_c}\right)^{-\nu}, \qquad 11.$$

where $\nu = 1/4$ and $\gamma = 1$. It should be noted that although these predictions may be satisfied in actual liquids at temperatures higher than T_c, they cannot be valid at temperatures close to or lower than T_c because no structural arrest is actually observed at T_c. Also, even if the predicted power-law growth of χ_4^p and ξ_d at temperatures higher than T_c is observed, the values of the exponents γ and ν are likely to be different from the mean-field values obtained in inhomogeneous MCT. The similarity of the predictions of inhomogeneous MCT with the behavior near continuous phase

transitions suggests that some of the numerical methods developed in studies of critical phenomena may be useful for obtaining quantitative information about the behavior of the length scale ξ_d, at least for temperatures higher than T_c.

The occurrence of DH also affects many other dynamic properties of supercooled liquids. The wide distribution of local relaxation times implied by DH causes the relaxation of density fluctuations to be nonexponential, leading to the stretched exponential decay of correlations found in the α-relaxation regime. Another consequence of DH is the breakdown of the Stokes-Einstein relation (see 43 and references therein) between the diffusion coefficient D and the viscosity η: $D\eta/T =$ constant, or equivalently, $D\tau =$ constant. It is believed that this behavior, also referred to as the decoupling of D and τ, is caused by the wide distribution of local relaxation times in supercooled liquids: Because D and τ reflect different moments of this distribution, their product does not remain constant as T is changed. From a numerical study of the breakdown of the Stokes-Einstein relation in a molecular liquid, Chong & Kob (44) have defined a characteristic length that may be related to the length scale of DH. They consider the timescale $\tau(k)$ obtained from the decay of the self-intermediate scattering function $F_s(k, t)$ for different values of k and examine whether the product $D\tau(k)$ remains constant as T is changed. They find that for sufficiently small values of k, $D\tau(k)$ remains constant over the temperature range considered, whereas for larger k, D decouples from $\tau(k)$ at a temperature that increases with increasing k. The value of k at which this decoupling occurs is then used to define a characteristic length l_{onset} (i.e., the onset length scale of Fickian diffusion) such that the relaxation time $\tau(k)$ decouples from D if $2\pi/k < l_{\text{onset}}$. The length scale l_{onset} is found to increase with decreasing T, indicating that the length scale beyond which the system looks homogeneous increases as T is decreased. The relation between this length scale and ξ_d has not been investigated in detail.

2.2. Mosaic Length Scale of Random First-Order Transition Theory and Point-to-Set Length Scales

We now consider proposals for static length scales that may be relevant for understanding the behavior of supercooled liquids. The most extensively studied proposals in this category are based on the RFOT theory originally proposed by Kirkpatrick et al. (45–52) and developed subsequently by many others (18). This theory is based on an analogy of the behavior of glass-forming liquids with that of mean-field Potts spin glass models and Ising spin glass models with multispin interactions. Exact analytic studies of these spin glass models with infinite-range interactions bring out a remarkable correspondence between their behavior and that of supercooled liquids. These models exhibit a dynamical transition to nonergodic behavior at $T = T_d$. The dynamics as T approaches T_d from above is described by the ideal version of MCT. The thermodynamic behavior for $T < T_d$ is governed by an exponentially large number of local minima of the free energy. A thermodynamic transition occurs at $T_s < T_d$ in which the configurational entropy per spin arising from the exponentially large number of free-energy minima goes to zero. These two temperatures are identified for structural glasses as the MCT transition temperature T_c and the Kauzmann temperature T_K.

Motivated by this similarity, Kirkpatrick et al. (52) argued that for a liquid below the MCT transition temperature T_c, there are an exponentially large number of metastable states (local minima of the free energy) that are statistically similar to one another. They also argued that the extensive configurational entropy arising from the presence of these metastable states causes a typical state of the system to have a mosaic structure in which different patches of the mosaic correspond to different metastable states. The mosaic length scale, defined as the typical linear dimension of these patches, was estimated from an argument in which the extensive

configurational entropy acts as a driving force for the nucleation of a droplet of a different metastable state in the background of one of these metastable states. For a compact droplet of size ξ, the entropy gain is given by $s_c(T)\xi^d$, where s_c is the configurational entropy per unit volume and d is the spatial dimension. The increase in energy due to the mismatch between the nucleating state and the parent state is estimated to be $\Upsilon\xi^\theta$, where Υ is a generalized surface tension and $\theta < (d-1)$ is an exponent that describes the dependence of the surface energy on the size of a droplet. The typical length of a nucleating droplet, obtained by equating these two contributions to the free energy, is given by $\xi_s = (\Upsilon/Ts_c(T))^{1/(d-\theta)}$. This length defines the mosaic length scale of RFOT theory. It diverges as the configurational entropy s_c goes to zero. A connection with the dynamics is established by assuming that the relaxation time τ corresponds to the timescale for thermal activation over the free-energy barrier for the nucleation of a droplet. This argument leads to a generalized Adam-Gibbs expression for the relation between the relaxation time and the configurational entropy:

$$\log\tau = \log\tau_0 + c\frac{\Upsilon}{k_BT}\left(\frac{\Upsilon}{Ts_c(T)}\right)^{\frac{\theta}{d-\theta}}, \qquad 12.$$

where c is a model-dependent constant. With the additional assumption that the configurational entropy s_c vanishes at temperature T_0 and the dependence of s_c on T near T_0 is linear, $TS_c(T) \propto (T - T_0)$, one arrives at the following generalized VFT form for the temperature dependence of τ:

$$\tau = \tau_0 \exp\left[\left(\frac{A}{T-T_0}\right)^{\frac{\theta}{d-\theta}}\right]. \qquad 13.$$

Kirkpatrick et al. (52) presented a scaling argument that suggests that the surface tension exponent $\theta = d/2$, leading to the original VFT relation.

The main drawback of the above picture is the lack of a clear explanation of the entropic driving force that leads to the nucleation of droplets. Bouchaud & Biroli (53) have presented a reformulation of the original arguments that provides a clearer definition of the mosaic length ξ. They consider one of the metastable states of the system, indexed by the label α, and assume that the motion of all particles outside a region $\mathcal{C}$ of linear dimension ξ is frozen. They then consider the thermodynamics of the inner region with the boundary condition imposed by the frozen outer particles. This boundary condition is a perfect match when the particles in the inner region are in the state α, and the energy is expected to be higher if the inner region is in some other state $\beta \neq \alpha$. This excess energy is assumed to have the same dependence on ξ (proportional to ξ^θ) as that of the surface energy in the original argument. This increase in energy tends to prevent the particles in the inner region from fluctuating into the other states. This is countered by the increase in entropy (proportional to ξ^d) that would occur if the particles in the inner region visit all the other metastable states. Given that $\theta < d$, the increase in energy is larger than the gain in entropy for small ξ, but the entropy dominates for sufficiently large values of ξ. Thus, there is a characteristic length ξ_s such that the inner region remains in state α for $\xi < \xi_s$ but explores the other states $\beta \neq \alpha$ if $\xi > \xi_s$. The dependence of ξ_s on s_c and the other parameters is the same as that in the original argument of Kirkpatrick et al. (52), but its physical interpretation is somewhat different. The length scale ξ_s in this interpretation is the largest linear dimension of a volume of particles that can be restricted to a single metastable state by the application of pinning boundary conditions. One can then argue that a macroscopic system must break up into a mosaic of metastable states with typical patch size given by ξ_s. If one further assumes that the energy barrier between different metastable states

grows with the length scale ξ as a power law with exponent ψ, then the typical equilibration time is obtained as

$$\tau(T) = \tau_0 \exp\left[\frac{\Delta_0 \xi_s^{\psi}}{k_B T}\right] = \tau_0 \exp\left[\frac{\Delta_0}{k_B T}\left(\frac{\Upsilon}{T s_c(T)}\right)^{\frac{\psi}{d-\theta}}\right]. \quad 14.$$

The values of the exponents θ and ψ are not known. As noted above, there exist heuristic agreements that suggest that $\theta = \psi = d/2$ (52).

The procedure described above to obtain the mosaic length ξ_s is analogous to that used to define the so-called point-to-set correlation functions in spin glasses (13). For this reason, the length scale ξ_s obtained from the Bouchaud-Biroli construction is also referred to as the point-to-set length scale. The term point-to-set is used to describe multipoint correlations determined by measuring the effects of fixing the positions of a set of particles on the probability of finding one of the other particles at a point. These correlations are expected to be very useful in the search for a static correlation length in supercooled liquids and other disordered systems because their definition does not rely on the assumption of any specific kind of structural order. In numerical studies of the point-to-set length scale, a spherical region of radius R is chosen in the system and all particles outside this region are frozen in one of the configurations obtained from an equilibrium simulation for the whole system. The particles in the spherical inner region are then allowed to equilibrate in the presence of the frozen outer region. For small values of the cavity size R, the particles in the cavity are expected to remain close to their original positions, whereas they should decorrelate from the initial state if R is sufficiently large. The length scale ξ_s at which this crossover occurs is obtained by measuring the average overlap of the particle configurations generated at equilibrium with the original one as a function of the cavity size R.

This method of obtaining the point-to-set correlation length has been generalized to include studies of the effects of other geometries of confinement. One of these generalizations (54) is to randomly choose a subset of the particles of a given equilibrium configuration and freeze their positions while the other particles are allowed to equilibrate in the random potential produced by the pinned particles. Kob et al. (55) have studied the effects of pinning the particles in the semi-infinite space ($z < 0$) on the particles in the $z > 0$ region. This geometry has the advantage that both dynamic and static effects induced by the frozen wall can be studied as a function of z. In **Figure 3**, four different geometries for pinning the particles are shown schematically. The first one is the box geometry, which is topologically identical to the spherical geometry mentioned before. The second one is the sandwich geometry, in which the fluid is confined between two frozen walls. The third one is the random pinning geometry, in which a fraction of particles are chosen randomly and their

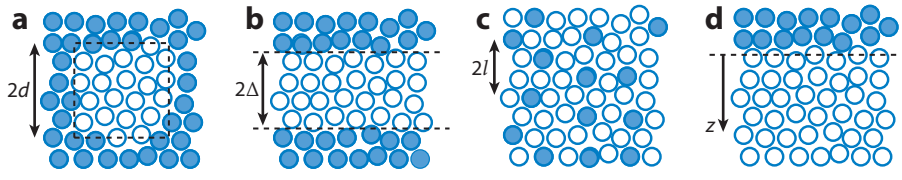

Figure 3

Schematic representation of four different geometries for extracting the point-to-set correlation length. In panel *a*, $2d$ is the linear size of the box (*indicated by the dashed square*) that contains the mobile regions. Similarly, 2Δ represents the distance between two frozen walls in panel *b*. In panel *c*, l represents the typical distance between two frozen particles, and z in panel *d* represents the distance from the frozen wall to the top. Adapted from Reference 56.

positions are frozen. The last one is the semi-infinite wall geometry, in which one side of the system is frozen and the effect of the wall is studied on the other side of the system. Results for ξ_s obtained from such studies are described in detail in Section 3.2.

2.3. Length Scale of Local Structural Order

The importance of local structural order in understanding the properties of supercooled liquids has been emphasized by Tanaka and coworkers (57–60) as well as by other researchers (61–63). Local patches of crystalline or other (e.g., icosahedral) order in the supercooled liquid, characterized by high bond-orientational order (64), led to the identification of a growing static length scale upon cooling the liquid, which is argued to be the cause of the rapid rise of relaxation times (58). In **Figure 4**, representative locally ordered regions (57) with high sixfold bond-orientational order in a typical configuration of a two-dimensional liquid are circled. The right panel illustrates the anticorrelation between bond-orientational order and the mean-square displacement of particles at an intermediate time τ_β. This anticorrelation implies that the heterogeneity in local dynamics is closely related to the local bond-orientational order. Results of similar studies in three-dimensional systems are less conclusive (65). An interesting observation (59) in this context is that the predominant local structural order in dense hard-sphere fluids in three dimensions has crystalline (face-centered cubic) symmetry, not the icosahedral symmetry proposed in earlier studies (64).

Although this description has several attractive features, there are reasons to believe that it is not universal in the sense that it does not explain the behavior of generic glass-forming liquids. There are several two-dimensional model liquids (66) in which the pronounced bond-orientational order shown in **Figure 4** is not found, but the dynamics exhibit a rapid growth of relaxation times. Also, the glass obtained by cooling or compressing a liquid with pronounced medium-range

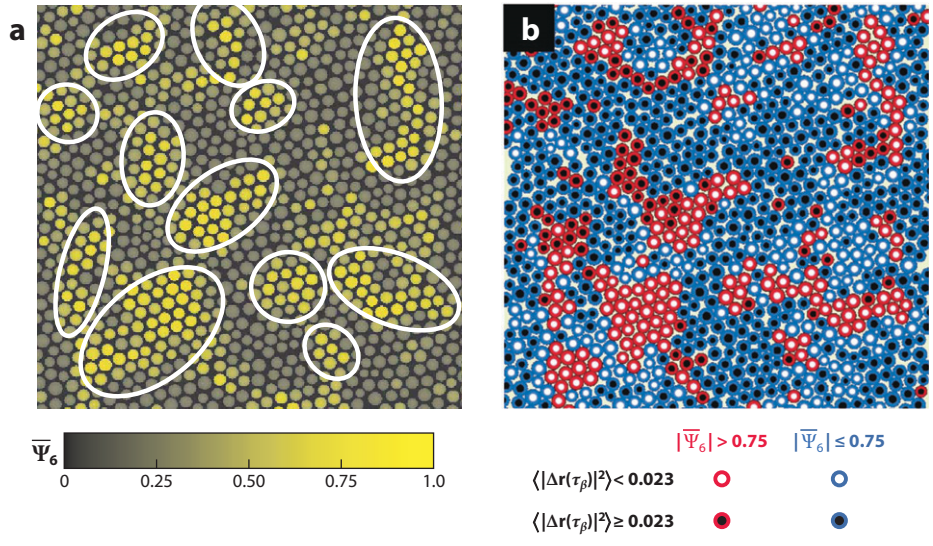

Figure 4

(*a*) Snapshot of a two-dimensional, polydisperse colloidal system at packing fraction $\varphi = 0.631$ and polydispersity $\delta = 9\%$, with the color map indicating the magnitude of the orientational order parameter $\overline{\Psi}_6$ averaged over the α-relaxation time. (*b*) Anticorrelation between bond-orientational order and the mean-square displacement of particles at an intermediate time.

crystalline order is expected to have a polycrystalline structure, not the amorphous structure found for generic glass formers. Further studies of the applicability of this description to a variety of glass-forming liquids would be most interesting.

2.4. Length Scale of Frustration-Limited Domains

Models that exhibit the formation of frustration-limited domains (67–71) were motivated by the expectation (64) that glassy behavior of liquids made of spherical particles may be understood from the tendency of these particles to form local icosahedral clusters, which leads to frustration at long length scales because such clusters cannot fill space. The growth of domains driven by short-range interactions are frustrated by the longer-range interactions, leading to frustration-limited domains with a size that may be viewed as a relevant static length scale that grows but does not diverge with decreasing temperature (67); the corresponding relaxation times show super-Arrhenius, but nondiverging, temperature dependence. The observed temperature dependence for many glass formers has been shown to be well described by the predicted form (68). The main drawbacks of this approach are (*a*) the nature and origin of the frustration-limited order that may develop in glass formers studied in experiments and simulations are not clearly understood, and (*b*) the observation that the local structural order in hard sphere–like systems in three dimensions is crystalline, not icosahedral (59), which argues against the idea of long-range frustrating interactions.

2.5. Patch Repetition Length

Another interesting proposal (72) for identifying and extracting a static length scale involves searching for repetitions of local patterns in particle configurations. The frequency of occurrence of patches of different sizes is proposed to be studied to identify a crossover length scale above which the entropy associated with patch repetitions becomes subextensive, whereas below this scale it is extensive. The authors of Reference 72 therefore propose a length scale associated with amorphous order, which may exist on a scale that could diverge at an ideal glass transition. These calculations have not been performed for any commonly studied model glass formers, and therefore we do not discuss these ideas at any greater length here. We return to them below in the context of discussing subextensive configurational entropies.

2.6. Length Scale Related to the Minimum Eigenvalue of the Hessian Matrix

From an analysis of how an amorphous solid behaves under external shear, it has been argued (73) that the density of vibrational states for an amorphous system exhibits an excess of low-frequency localized modes that are not present in corresponding crystalline materials. The well-known boson peak (74) in the vibrational spectrum of amorphous systems is supposed to be a manifestation of these excess modes. These modes are believed to be responsible for structural relaxation in glassy systems. In Reference 73, the vibrational spectrum in the harmonic approximation was obtained from a calculation of the eigenvalues of the Hessian matrix at local minima of the potential energy (the so-called inherent structures) of model glass formers. It was realized that the low-frequency modes can be divided into two families: One corresponds to the Debye model of an elastic solid and the other is that of localized modes that are responsible for irreversible plastic events in the system. These modes are referred to as plastic modes in the following discussion.

The main idea behind the analysis is to estimate the number of these plastic modes in the system at a given temperature to extract a density of disorder at that temperature. A characteristic static

length scale can then be defined as the inverse of the cube root (square root) of the disorder density for three-dimensional (two-dimensional) systems. As these considerations apply to the low-frequency modes, the analysis was done for the lowest frequency in the spectrum, and it was shown (73) that the lowest frequency is a scaling function of the underlying static length scale. A detailed finite-size scaling analysis was performed to extract the static length scale for various temperatures. The results obtained from this approach are described in detail in Section 3.2.

2.7. Length Scale of Nonaffine Deformations

On the basis of the nonequilibrium thermodynamic formulation of the glass transition (75, 76), Mosayebi et al. (77) have proposed another way of extracting a static length scale. The idea behind this method is to compare two inherent structures obtained by minimizing the potential energy starting from two initial states related to each other by a static shear transformation. The nonaffine part of the displacement field that measures the difference in particle positions at the two inherent structures shows interesting spatial correlation. In Reference 77, a growing correlation length was extracted from these correlations. The relation of this length scale with the others discussed above is not clear at present.

2.8. Length Scale Related to the Extensivity of the Configurational Entropy

In Reference 38, the system-size dependence of the configurational entropy per particle was used to define a static length scale that characterizes the crossover from extensive to subextensive dependence of the configurational entropy on system size. It was shown that this length scale exhibits much weaker temperature dependence than the length scale of DH. The relationship of this length scale with other static length scales is discussed in Section 3.

3. SUMMARY OF AVAILABLE RESULTS

In this section, we summarize the currently available results for the various dynamic and static length scales discussed in the preceding section. Nearly all of these results are obtained from numerical simulations because the procedures used for estimating most of the length scales mentioned above are very difficult (if not impossible) to implement experimentally [some experimental results are available for a dynamic susceptibility closely related to the length scale of DH (78, 79)]. Because simulations are restricted to relatively small length and timescales, it is sometimes difficult to draw clear conclusions from the numerical results. As discussed below, these limitations have hampered the development of a better understanding of length scales in supercooled liquids.

3.1. Results for Dynamic Length Scales

The most commonly studied dynamic length scale in supercooled liquid is that of DH. The earliest studies of the length scale of DH were carried out by Hurley & Harrowell (80) and Yamamoto & Onuki (81). Hurley & Harrowell measured a correlation length based on how the variance of the block average relaxation times depends on the block size of averaging. Yamamoto & Onuki labeled bonds that had broken after a specified elapsed time, constructed a structure factor for the broken bonds and analyzed it by assuming an Ornstein-Zernike form, thus anticipating much work in evaluating length scales that has been undertaken more recently.

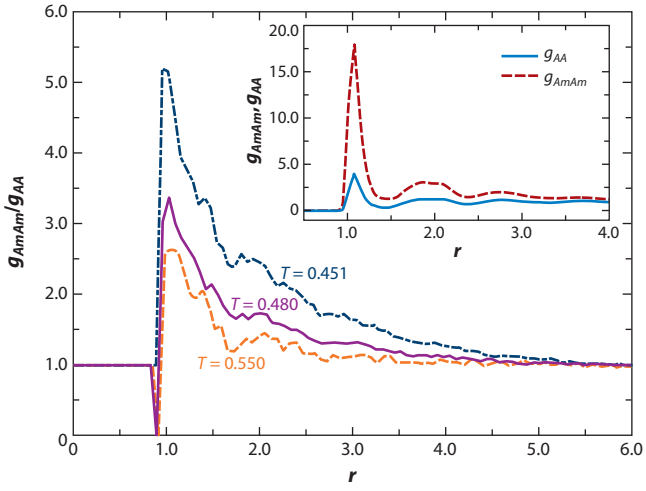

Figure 5

Spatial correlation function of mobile particles, showing that correlations are present and grow upon lowering the temperature. Inset: radial distribution functions $g_{AmAm}(r)$ and $g_{AA}(r)$ for the mobile and bulk particles, respectively, for $T = 0.451$. Main figure: Ratio between $g_{AmAm}(r)$ and $g_{AA}(r)$ for $T = 0.550$, $T = 0.480$, and $T = 0.451$ (temperatures are given in reduced units). Adapted from Reference 23.

Similarly to the pair correlation function $g(r)$, which is based on particle positions, a correlation function of mobile particles $g_{MM}(r)$ can be defined. Numerical results for $g_{MM}(r)$, normalized with the full $g(r)$, are shown in **Figure 5**. This function provides information about spatial correlations of mobile particles (23). It is apparent that such a correlation exists and grows upon lowering the temperature. Poole et al. (82) defined an excess displacement-displacement correlation function along the same lines, and assuming an exponential decay of correlations, they obtained a correlation length that grows as the temperature is lowered.

As already mentioned, the four-point susceptibility $\chi_4(t)$, the corresponding length scale ξ_d, and their relationship with structural relaxation times have been of central importance to many recent studies (35–38, 40, 83). In this context, the use of finite-size scaling (38, 84) has been very useful in estimating a heterogeneity length scale as well as in elucidating the finite-size dependence of dynamics, which is of intrinsic interest. In the finite-size scaling method (85), with the assumption of the existence of a characteristic length scale determining the properties of the system, quantities of interest are measured in simulations for systems of several finite sizes. By assuming a scaling form for the size dependence of the quantities, finite-size data is used to extract the characteristic length scale at desired state points. This method has been used recently (38) to obtain definitive results for the growth of ξ_d in a simple model liquid (86). The left panel of **Figure 6** shows the temperature dependence and system-size dependence of χ_4^p, the peak value of $\chi_4(t)$. It is observed that χ_4^p initially increases with system-size N for small values of N and eventually saturates for large N, as may be expected of a susceptibility in conventional critical phenomena. The susceptibility per particle, χ_4^p, is expected to depend on N only if the linear size of the system, $L \propto N^{1/d}$ (d is the spatial dimension), is comparable to or smaller than the relevant correlation length ξ_d. Because the N-dependence of χ_4^p shown in the left panel of **Figure 6** persists to larger values of N at lower temperatures, these results imply the existence of a correlation length that increases as T is decreased.

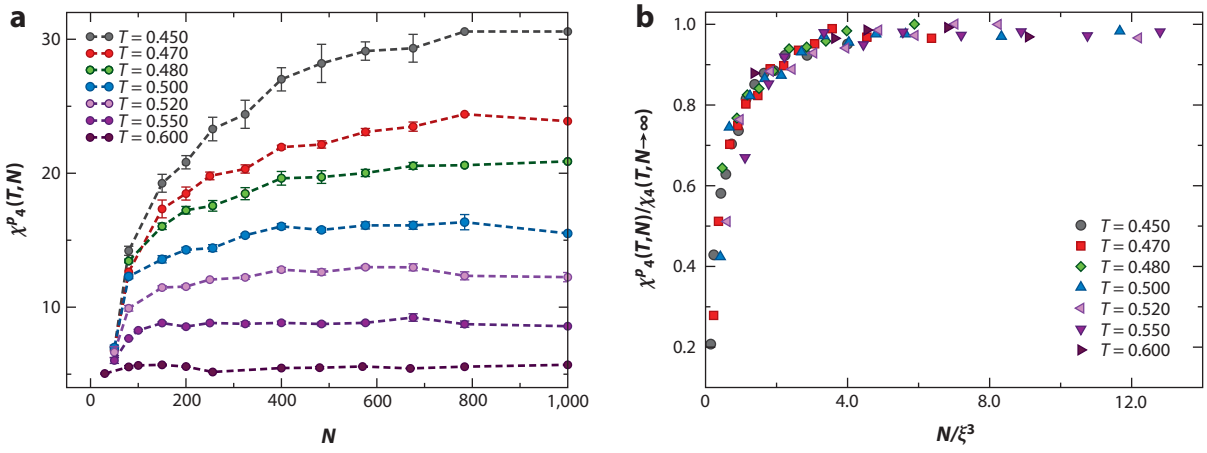

Figure 6

(*a*) Variation of the four-point susceptibility, $\chi_4^p(T,N)$, of a three-dimensional binary Lennard-Jones system, with the system-size N for different temperatures. (*b*) Scaling collapse of the data shown in panel *a*, using the dynamic length scale $\xi_d(T)$. Adapted from Reference 38.

According to the finite-size scaling hypothesis (85), the system-size dependence of χ_4^p is expected to have the form

$$\chi_4^p(T,N) = \chi_4^p(T,N\to\infty) g_\chi\left[L/\xi_d(T)\right]. \qquad 15.$$

Therefore, the data for all T and N should collapse to the same scaling curve in a plot of $\chi_4^p(T,N)/\chi_4^p(T,N\to\infty)$ versus $L/\xi_d(T)$ [or, equivalently, $N/\xi_d^d(T)$] for the correct choice of the values of $\xi_d(T)$ at different temperatures. A scaling collapse of the data for $\chi_4^p(T,N)$ is shown in the right panel of **Figure 6**. From this and a similar analysis of the data for the Binder cumulant (85) obtained from the distribution of the overlap $\tilde{Q}(t)$, it was found (38) that ξ_d grows from ~2 to ~6 (in reduced units for Lennard-Jones systems) as the temperature is reduced from 0.7 to 0.45 (the critical temperature T_c of MCT is 0.435 in this system).

Another method borrowed from studies of critical phenomena to estimate length scales involves an analysis of the k-dependence of a four-point structure factor, $S_4(k,\tau_4)$, defined as

$$S_4(k,\tau_4) = \left\langle \left| \sum_{i=1}^{N} e^{i\mathbf{k}\cdot\mathbf{r}_i(0)} w\left(\left|\mathbf{r}_i(0) - \mathbf{r}_i(\tau_4)\right|\right) \right|^2 \right\rangle. \qquad 16.$$

In systems with a large correlation length, ξ_d, the k-dependence of this quantity for small k is expected to follow the Ornstein-Zernike form given by

$$S_4(k,\tau_4) = \frac{\chi_4(\tau_4)}{1+k^2\xi_d^2}. \qquad 17.$$

Therefore, the value of ξ_d may be obtained by fitting numerical data for $S_4(k,\tau_4)$ to this form for small k.

Although Ornstein-Zernike fits to the four-point structure factor have been used extensively, reliable estimation of correlation lengths from this approach is difficult (87, 88). It was shown by

Karmakar et al. (88, 89) that the estimates of the length scale were subject to large system-size effects, and one needed to access rather small wave vector values in order to obtain accurate results for the heterogeneity length scale. One reason for this is the intricate ensemble dependence (36, 40) of the four-point susceptibility, which forms the $q \to 0$ limit of the four-point structure factor $S_4(q, t)$: This limiting value may not be the same as the directly calculated $S_4(q = 0, t)$ in certain ensembles. The results obtained for ξ_d from simulations of very large systems (89) were found to be the same as those obtained earlier from finite-size scaling (38), thereby providing a reliable estimate of ξ_d for T higher than the MCT T_c. The value of the exponent ν defined in Equation 11 was found to be close to 2/3, which is quite different from the prediction $\nu = 1/4$ of inhomogeneous MCT (39, 40). Similar results for ξ_d have been obtained in several other recent studies (35–37).

A different dynamic length scale has been obtained from a study of the effects of boundary conditions on the local dynamics (55). The boundary considered in this work is shown in **Figure 3*d***. The local dynamics are then studied as a function of the distance from the wall, and a length scale is extracted from the observed exponential decay of the effect of the wall on the local dynamics. Surprisingly, it was found that this length scale grows with decreasing T for $T > T_c$ but saturates and eventually decreases as T is further reduced below T_c. A recent calculation (90) of ξ_d from $S_4(q, t)$ for a different model system does not show a similar nonmonotonic behavior of this length scale near T_c. It appears that the length scale obtained in Reference 55 is different from ξ_d. The physical significance of this length scale is not clear at present.

3.2. Results for Static Length Scales

Most attempts to compute the mosaic or point-to-set length scale ξ_s have been based on the Bouchaud-Biroli procedure described above. The main problem in implementing this procedure is that it is very difficult to equilibrate the particles in the spherical inner region at low temperatures using standard molecular dynamics or Monte Carlo methods. This procedure was first implemented by Biroli et al. (91) for a binary mixture interacting via an inverse power-law potential. The numerical difficulty in equilibrating the particles in the inner region at low temperatures was partially overcome by using a Monte Carlo swapping method developed in Reference 92. In order to extract the static length scale, an overlap function $q_c(R)$ was calculated in the central part of the spherical inner region of radius R. To define $q_c(R)$, the simulation box was divided into small cells of size l such that the probability of finding more than one particle in a single cell is negligibly small. The variable n_i that denotes the number of particles in cell i then takes the value 0 or 1. In terms of these variables, the overlap function is defined as

$$q_c(R) = \frac{1}{l^3 N_\nu} \sum_{i \in \nu} \langle n_i(t_0) n_i(t_0 + \infty) \rangle, \qquad 18.$$

where the sum runs over all the cells within the volume ν at the center of the sphere, N_ν is the number of such cells, $l^3 N_\nu$ is the number of particles in the volume ν, and $\langle \ldots \rangle$ represents both thermal averaging and averaging over different realizations of the frozen boundary. The function is normalized in such a way that two identical configurations have overlap equal to unity and two uncorrelated random configurations have overlap close to $q_0 = l^3$. In **Figure 7*a***, $q_c(R) - q_0$ is plotted as a function of R for four different temperatures. One can see that at high temperatures, the function decays nearly exponentially with R, but as the temperature is lowered, the decay becomes slower and also the nature of the decay changes. This behavior was attributed to the growth of the static length scale with decreasing temperature. As shown in the inset of the figure, $q_c(R) - q_0$ calculated for the whole sphere decays more slowly with R in comparison to that defined only in the central region. This is due to strong boundary effects in the overlap calculated for the whole sphere.

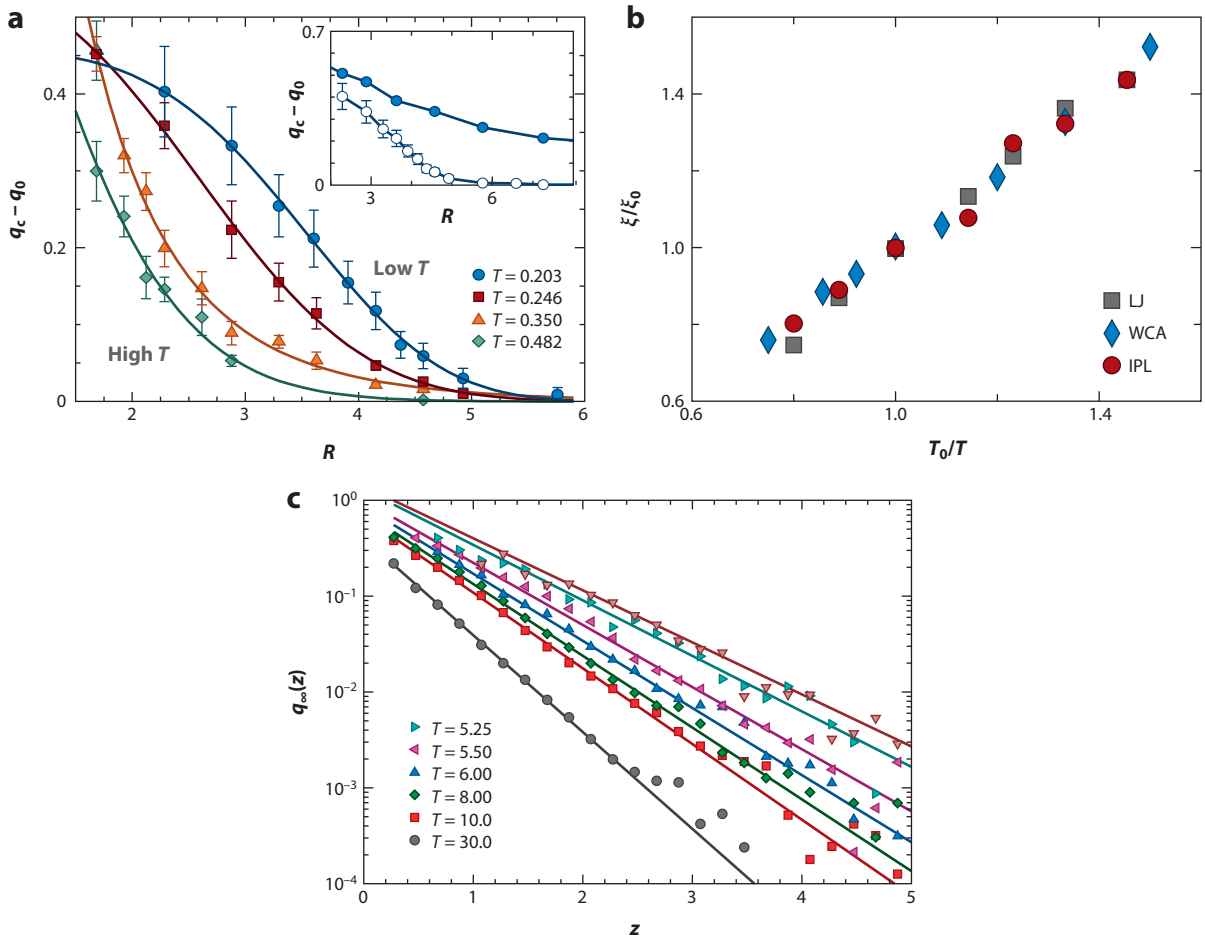

Figure 7

(*a*) The overlap $qc - q0$ as a function of cavity radius R for different temperatures. A slower decay of this function indicates a larger value of the point-to-set length scale. Adapted from Reference 91. Inset: Comparison of $q_c - q_0$ at $T = 0.203$ (*open circles*) with the overlap integrated over the whole sphere (*filled circles*). (*b*) The extracted point-to-set length scales for different model systems. See Reference 93 for further details. Abbreviations: IPL, inverse power law; LJ, binary Lennard-Jones; WCA, Weeks-Chandler-Andersen. (*c*) The overlap as a function of the distance z from the wall for different temperatures for the geometry shown in panel *d* of **Figure 3**. The overlap decays more slowly with decreasing temperature, indicating the growth of a static length scale. Adapted from Reference 56.

The dependence of $q_c(R) - q_0$ on R at low temperatures was found to be well described by the compressed exponential form

$$q_c(R) - q_0 = \Omega \exp\left[-(R/\xi)^x\right], \qquad 19.$$

where $x \geq 1$. It was argued that this behavior arises from fluctuations in the surface tension Υ that appears in the RFOT theory and the value of ξ obtained from a fit of the data to this form was taken to be the static length scale ξ_s. The value of ξ_s was found to increase from ~0.6 to ~3.8 (in units of average interparticle distance) in the temperature range considered in this work. The lowest temperature considered in this study was below the MCT T_c.

Subsequently, it was realized that the method used in Reference 91 to equilibrate the system at low temperature is not very general and cannot be used effectively for other glass-forming models. Hocky et al. (93) have developed an improved Monte Carlo algorithm that can be used effectively for different models to equilibrate the system in the spherical cavity geometry. Using this method, they were able to calculate the length scale ξ_s for different glass-forming liquids and compare how this length scale grows with decreasing temperature, as shown in **Figure 7*b***. The change in the length scales found here is smaller than that found in Reference 91 because the temperatures considered in this study are higher than the MCT critical temperatures of the models considered.

Kob et al. (55) have considered a different geometry in which equilibration was not severely hampered. They studied the effect of a wall (the geometry shown in **Figure 3*d***) on the dynamic and equilibrium behavior as a function of distance from the wall. An overlap function similar to that defined above was used to extract a static length scale from the observed dependence on the distance from the wall. In **Figure 7*c***, the overlap is shown as a function of the distance z from the wall for different temperatures. It is clear that the overlap decays more slowly with decreasing temperature, indicating the growth of a static length scale. The other pinning geometries shown in **Figure 3** have also been considered in a recent study (56), where it was found that the static length scale extracted from the data depends to some extent on the pinning geometry. The reason for this dependence is not clear at present.

It was mentioned earlier that the point-to-set length scale can also be calculated using the random pinning geometry shown in **Figure 3*c***. This geometry has been used by Charbonneau and coworkers (94, 95) to calculate the point-to-set length scale in binary hard-sphere systems. For a system with a fraction c of particles pinned at their positions in an equilibrium configuration, an overlap function was defined as follows:

$$Q_c(t) = \frac{1}{(1-c)^2 N} \left\langle \overline{\sum_{i,j} w_{ij}(0,t)} \right\rangle, \qquad 20.$$

where $w_{ij}(0,t) = \Theta(a - |\mathbf{r}_i(t) - \mathbf{r}_j(0)|)$, $\Theta(x)$ is the Heaviside step function, and $a = 0.30$ in the unit of particle diameter. The angular brackets represent equilibrium averaging, the overbar means averaging over different ways of pinning a fraction c of the particles, and the sum runs over all the unpinned particles. If the static length scale is larger (smaller) than the typical distance between two pinned particles, then the asymptotic overlap $Q_c(\infty) = Q_c(t \to \infty)$ should be large (small). Therefore, the static length scale can be extracted from the crossover of the asymptotic overlap $Q_c(\infty)$ as a function of the pinning fraction c.

In the left panel of **Figure 8**, the overlap $Q_c(\infty)$ (after subtracting the value for two completely uncorrelated configurations) is plotted as a function of the average distance between neighboring pinned particles. One can see that as the density of the system increases, the crossover from high to low values of the overlap occurs at a lower concentration of the pinned particles, indicating the increase in the static length scale. In the right panel of **Figure 8**, the static length scale, defined somewhat arbitrarily as the value of the average interpin distance at which the overlap difference is equal to 0.4 (indicated by the dashed line in the left panel), has been plotted as a function of the reduced pressure. The growth of the corresponding dynamic length scales is also shown in the same figure. The dynamic length scale is found to grow more rapidly with increasing density than the static length scale in this regime of density.

A very different method was used in Reference 38 to obtain a static length scale for the Kob-Andersen model in three dimensions. It was found in that work that the configurational entropy per particle (s_c) of the collection of inherent structures exhibits a weak dependence on the system-

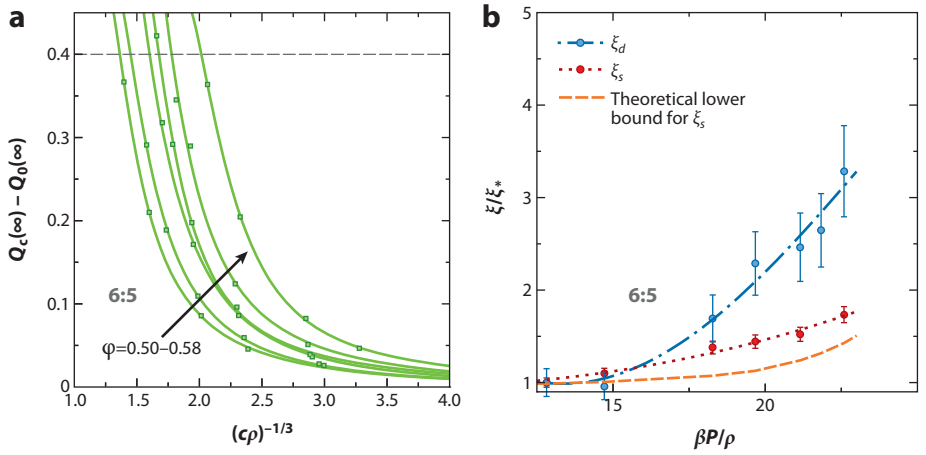

Figure 8

(*a*) The overlap function calculated for a three-dimensional hard-sphere binary mixture for the random pinning geometry shown in panel *c* of **Figure 3**. (*b*) The growth of the extracted static length scale ξ_s for this system (*red symbols*). Note the rapid growth of the corresponding dynamic length scale ξ_d (*blue symbols*) compared to the slow growth of ξ_s. Adapted from Reference 95.

size N [$s_c(T, N)$ increases with increasing N] for relatively small values of N. According to the finite-size scaling hypothesis (85), this N-dependence should be described by the scaling form

$$s_c(T,N)/s_c(T,N\to\infty) = g_s\left[N/\xi^d(T)\right], \qquad 21.$$

where $\xi(T)$ is a static length scale and g_s is a scaling function. The data for $s_c(T, N)$ were found to be consistent with this scaling form, with a choice of $\xi(T)$ that increases slowly with decreasing temperature.

Results for the static length scale obtained from the smallest eigenvalue of the Hessian matrix are shown in **Figure 9**. These results were obtained for the three-dimensional Kob-Andersen model. The left panel shows the ensemble average of the smallest eigenvalue rescaled by the corresponding Debye value (square of the Debye frequency) as a function of an appropriate scaling variable (73) for different temperatures. The right panel shows that good data collapse is obtained by appropriately choosing the static length scale. The inset of the right panel shows the growth of this static length scale with decreasing temperature. In Reference 73, it was also shown that the temperature dependence of this length scale agrees very well with that of the length scale obtained from a finite-size scaling analysis of the dependence of the configurational entropy on system size.

The static length scales obtained in all of the studies described above are quite small, on the order of a few interparticle distances. Also, they grow only by a factor of ~2 in the temperature range accessible in simulations. All these studies, except for that found in Reference 91, have been carried out at temperatures above the characteristic temperature T_c of MCT. The physics described by the RFOT theory is expected to be relevant for temperatures close to and lower than T_c. Therefore, it is perhaps not surprising that the values of the mosaic or point-to-set length scale ξ_s are small in this temperature range. It would, of course, be very interesting to extend these studies to lower temperatures to investigate the growth of ξ_s. Given the very limited range of the growth of the static length scales in the studied temperature range, it is not meaningful to inquire whether this growth is quantitatively described by one of the existing theories. It is, however, meaningful to ask

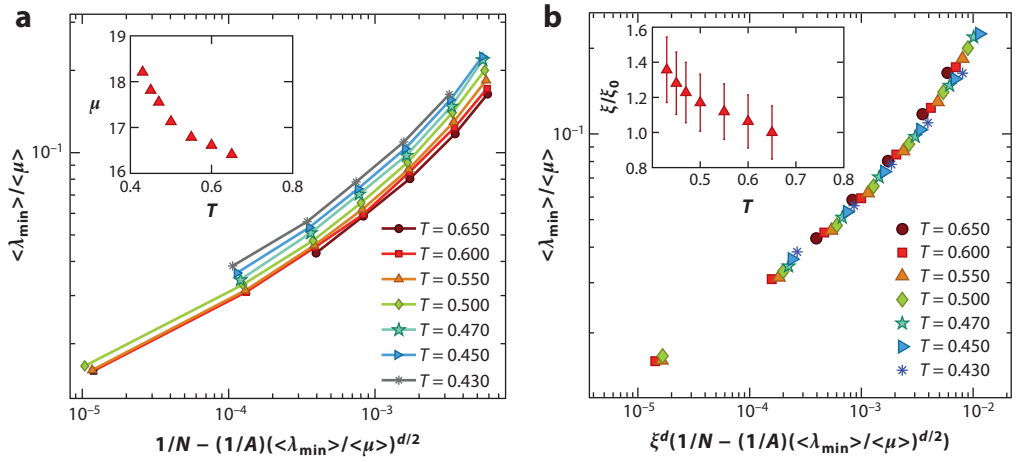

Figure 9

(*a*) The ensemble average of the smallest eigenvalue, rescaled by the corresponding Debye value (square of the Debye frequency), as a function of an appropriate scaling variable (73) for different temperatures. (*b*) The data collapse obtained by appropriately choosing the static length scale. The inset shows the growth of this static length scale with decreasing temperature. Adapted from Reference 73.

whether different systems exhibit similar dependence of the static length scale on temperature. A simple way to address this question is to choose a suitable reference temperature T_0 for each system using a physical criterion (e.g., T_0 could be the temperature at which the length scale has the same value for all of the considered systems) and then plot the scaled length $\xi(T)/\xi(T_0)$ as a function of the scaled temperature T/T_0. If the plots for different systems collapse into the same curve, then it is reasonable to conclude that the temperature dependences of ξ in the different systems are similar. **Figure 7*b*** shows such a plot for three different systems. The data collapse indicates a degree of universality in the growth of the length scale ξ_s with decreasing temperature.

Another important question is whether the different methods for estimating the static length scale lead to results that agree with one another. An answer to this question is not yet available because all the different methods for calculating the static length scale have not been applied to the same model system. The Kob-Andersen model is the only system for which results for the static length scale have been obtained using more than one method. The lowest eigenvalue method and finite-size scaling of the configurational entropy yield (73) the same results in this system. There are also indications (96) that the point-to-set length in this system is the same as these two length scales.

The dependence of the configurational entropy $s_c(T, N)$ on the system-size N for relatively small values of N poses the following potential problem in defining the mosaic length of RFOT theory. The prescription used in RFOT theory to obtain the mosaic length assumes that the total configurational entropy is extensive: The entropy of a droplet of size ξ is taken to be $s_c\xi^d$ with s_c independent of ξ. If s_c itself depends on the droplet size ξ, as would be the case if ξ is sufficiently small, then the expression for the mosaic length ξ_s given in Section 2.2 must be corrected to take into account this dependence. The corrected expression would be $\xi_s = \left(\Upsilon/Ts_c\left(T, \xi_s^d\right)\right)^{1/(d-\theta)}$, which appears to be a complicated implicit equation for ξ_s. However, if the dependence of the configurational entropy on the system size is given by Equation 21, with ξ identified with the mosaic scale ξ_s, then the simple expressions given in Section 2.2 would be recovered with Υ replaced by Υ/G, with $G \equiv g_s(1)$ being a constant of order unity and $s_c(T) = s_c(T, N \to \infty)$. Thus, all the predictions of RFOT theory would be correct if the mosaic length were the same as the length

scale that describes the dependence of s_c on system size. As mentioned above, there is some numerical evidence suggesting that these two length scales are indeed the same.

3.3. Relation Between Static and Dynamic Length Scales

A close relation between structure and dynamics exists in most condensed matter systems. It is, therefore, natural to expect that the dynamic and static length scales in supercooled liquids should be related to each other. Because the dynamic length scale that has received the most attention in the literature is that of DH, it is important to understand whether there is a structural basis for the occurrence of DH. This question has been addressed in many studies, but a clear answer is still not available. Several numerical (97–99) and experimental (100 and references therein) studies have pointed out a close connection between the spatial structure of DH and that of the eigenvectors of low-frequency eigenmodes of the dynamical matrix that describes the vibrational spectrum of the system. However, quantitative information such as the existence of a characteristic (static) length scale has not been extracted from the structure of these low-lying modes. A comparison of the behavior of static and dynamic length scales calculated for the same system is expected to provide valuable insights into this question.

Surprisingly, all existing studies (38, 55, 56, 93–95) in which both static and dynamic length scales have been computed for the same system indicate that these length scales are not related to each other. The dynamic length scale ξ_d is larger than the static scale ξ_s, and it increases faster with decreasing temperature in the temperature range in which numerical results are available (see the right panel of **Figure 8** for an example of this behavior). This is similar to the behavior found by Franz & Montanari (101) in an analytic calculation of both the static (mosaic) length scale and the dynamic length scale associated with the four-point density correlation function for a Kac model with finite-range interactions. This calculation shows that both length scales exist at all temperatures and are unrelated to each other. The dynamic length scale diverges at a dynamic transition temperature T_d, and the static length scale diverges at a lower temperature T_s, meaning that the dynamic length scale is much larger than the static length scale at temperatures close to T_d. In real liquids, the dynamic transition at T_d is supposed to be replaced by a crossover at the MCT temperature T_c. Therefore, the dynamic length scale is expected to be the larger one at temperatures close to T_c, with the possibility that the static length scale will become large (perhaps larger than the dynamic one) as the temperature is decreased below T_c. This scenario is consistent with the available results, but the behavior at temperatures substantially below T_c remains unclear at this time.

4. RELATION BETWEEN LENGTH SCALES AND TIMESCALES

Because the rapid growth of timescales is the defining feature of glass transition, the most important question that should be addressed in studies of length scales is whether the growth of the length scale being considered can explain the growth of timescales. Given that many different timescales are present in glassy relaxation, it is necessary to decide which timescale should be considered in this context. The α-relaxation time τ extracted from the long-time decay of density correlation functions, such as those defined in Equations 7, 8, and 10, is the most extensively studied timescale in glassy dynamics. This timescale is proportional to the time at which the four-point susceptibility $\chi_4(t)$ peaks, but it is different from (larger than) the time t^* at which the non-Gaussian parameter $\alpha_2(t)$ peaks (27). The strings formed by cooperatively moving mobile particles (see Section 2.1) reach maximum size on a timescale that is proportional to t^*, and as recently discussed by Starr et al. (27), t^* is characteristic of diffusion, and it scales with D/T, where D is the

diffusion coefficient and T is the temperature. Mobile particle clusters are found (27, 102, 103) to have the largest sizes at a timescale that is also proportional to t^*, whereas immobile particle cluster sizes peak at a time that is proportional to the α-relaxation time τ. Thus, immobile particle clusters are associated with structural relaxation, which occurs on a different (larger) timescale than diffusion timescales that scale as t^*. The timescale that characterizes the lifetime of fluctuations (37) of the overlap function $\tilde{Q}(t)$ is different from both t^* and τ. We concentrate here on the α-relaxation time τ.

To establish a direct relation between τ and a specific length scale ξ, it is necessary to measure both τ and ξ for different systems and to demonstrate that the relation between τ and ξ changes in a systematic and predictable way from one system to another. This is how the relation between the relaxation time and the correlation length was established in standard critical phenomena. However, the kind of universality observed in critical phenomena is not expected to be present in the glass transition problem because the correlation lengths in supercooled liquids cannot be very large in the temperature range that is accessible in experiments and simulations. This is a consequence of the fact that the lowest temperature ($\simeq T_g$ or T_c) at which the liquid can be equilibrated in experiments or simulations is significantly higher than the temperature ($T_0 \simeq T_K$) of the putative critical point. This makes it difficult to compare the relation between τ and ξ obtained for systems with different microscopic Hamiltonians. It is not clear how the differences in the microscopic length scales and timescales in the systems being considered should be taken into account. The method of finite-size scaling does not have this problem because the systems of different size considered in this method have the same microscopic interactions. This method was used in Reference 38 to investigate whether the timescale τ is causally related to the length scale ξ_d of DH in the Kob-Andersen model. As discussed in Section 3.1, the system-size dependence of the four-point susceptibility χ_4^p in this model was found to be well-described by the finite-size scaling form of

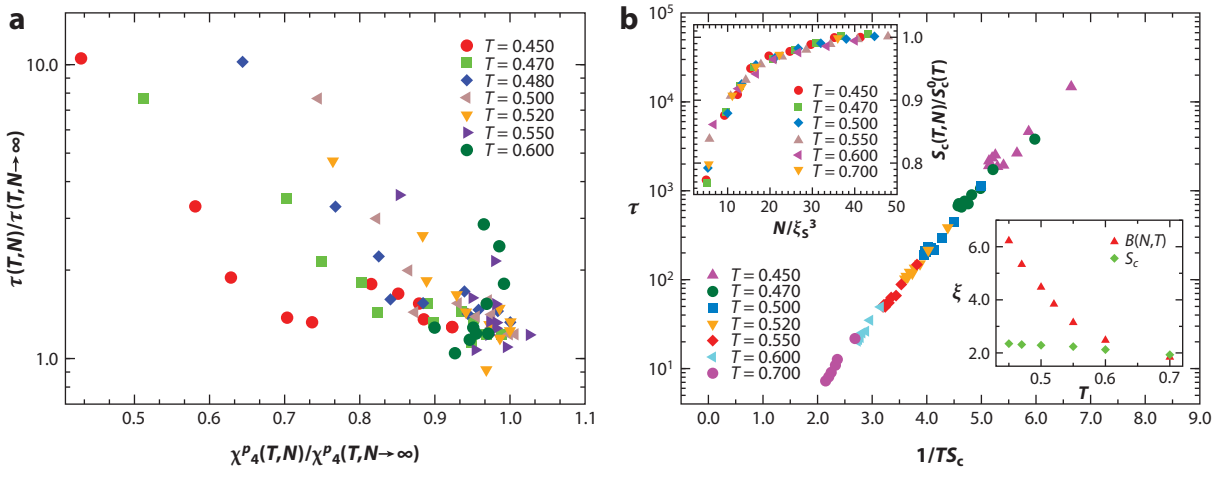

Figure 10

(*a*) Relaxation times for different system sizes rescaled by the large system-size value are plotted versus the corresponding peak values of the four-point susceptibility rescaled by the values in the large system-size limit for the three-dimensional Kob-Andersen model. The scatter of the data implies that the length scale which governs the growth of the four-point susceptibility does not govern the growth of the relaxation time. (*b*) Validation of the Adam-Gibbs relation. Relaxation times for different system sizes and temperatures fall on a master curve when plotted as a function of $1/(TS_c)$, as in the Adam-Gibbs relation, Equation 2. The top inset shows finite-size scaling data collapse for the configurational entropy $s_c(T, N)$. The temperature dependence of the extracted static length scale and its comparison with the dynamic length scale ξ_d are shown in the bottom inset. Adapted from Reference 38.

Equation 15. If the growth of τ with decreasing temperature is also governed by the same length scale ξ_d and τ exhibits normal dynamic scaling, then the system-size dependence of $\tau(T, N)$ should also be described by a similar scaling form with a different scaling function. This, in turn, implies that a plot of $\tau(T, N)/\tau(T, N \to \infty)$ versus $\chi_4^p(T, N)/\chi_4^p(T, N \to \infty)$ for different T and N would collapse to a single master curve. It was shown in Reference 38 that such a scaling collapse of the data does not occur. The dependence of τ on N is qualitatively different from that of χ_4^p: The timescale decreases with increasing N for small N, whereas the susceptibility is an increasing function of N. As shown in the left panel of **Figure 10**, a plot of $\tau(T, N)/\tau(T, N \to \infty)$ versus the ratio $\chi_4^p(T, N)/\chi_4^p(T, N \to \infty)$ does not show any sign of a scaling collapse.

This observation strongly suggests that the growth of the relaxation time τ in the studied temperature range is not determined primarily by the DH length scale ξ_d that governs the behavior of χ_4^p. This surprising conclusion has been corroborated in a recent study (93) that concluded that growth of the relaxation time is not strongly correlated with that of the DH length scale.

It was also shown in Reference 38 that the data for the configurational entropy $s_c(T, N)$ and $\tau(T, N)$ satisfy the Adam-Gibbs relation of Equation 2 for all T and N. This is shown in the right panel of **Figure 10**. This observation implies that the growth of the relaxation time τ is governed by the static length scale obtained from the finite-size scaling of $s_c(T, N)$. The top inset of the right panel of **Figure 10** shows finite-size data collapse for the configurational entropy $s_c(T, N)$. The temperature dependence of the extracted static length scale and its comparison with the dynamic length scale ξ_d are shown in the bottom inset.

As noted above, this static length scale has been found to be identical to that obtained from the lowest eigenvalue of the Hessian matrix (104). The connection between τ and this static length scale ξ_s has been demonstrated explicitly in Reference 105 from a finite-size scaling analysis of τ itself.

In the left panel of **Figure 11**, the system-size dependence of the relaxation time τ is shown for several temperatures. One can clearly see that the system-size dependence of τ becomes more

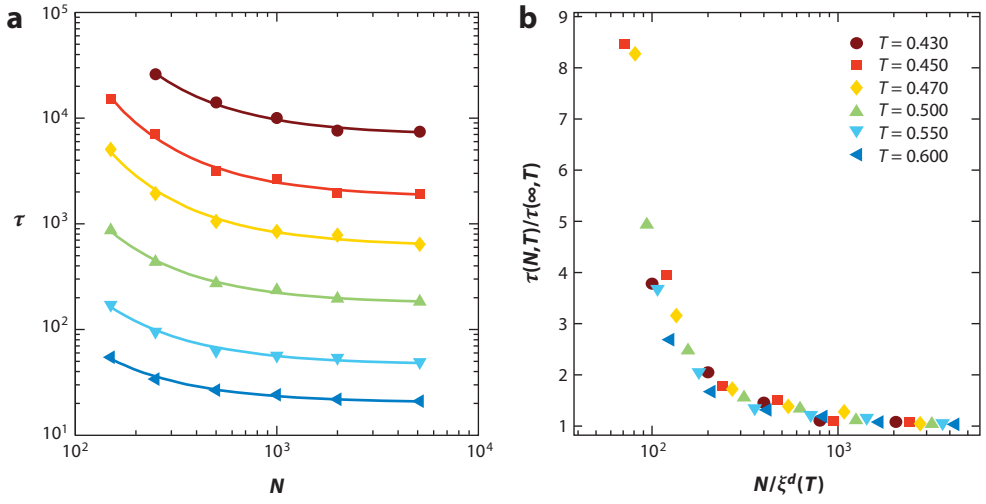

Figure 11

(*a*) The system-size dependence of the relaxation time for different temperatures in the three-dimensional Kob-Andersen model. Note the enhanced system-size dependence at lower temperatures. (*b*) The data collapse obtained using the static length scale obtained from the finite-size scaling analysis of the minimum eigenvalue of the Hessian matrix. Adapted from Reference 105.

pronounced at lower temperatures. The right panel of this figure shows a scaling collapse of the data into a single master curve using the length scale obtained from the finite-size scaling of the minimum eigenvalue of the Hessian matrix. The relevance of this static length scale in the growth of τ was demonstrated in another calculation (104) in which the random pinning geometry mentioned above was used. If a fraction ρ_{im} of the particles are pinned at their positions in an equilibrium configuration, then the typical distance between two neighboring pinned particles is proportional to $\rho_{im}^{-1/d}$, where d is the spatial dimension. If the system has a relevant length scale ξ_s, then the dependence of observables on the pin density ρ_{im} should be governed by the dimensionless scaling variable $\xi_s \rho_{im}^{1/d}$ or, equivalently, by $\xi_s^d \rho_{im}$. It has been shown in Reference 104 that the dependence of τ on T and ρ_{im} is indeed well described by this scaling hypothesis, with ξ_s equal to the length scale extracted from the minimum eigenvalue of the Hessian matrix.

Similar results for the importance of the static point-to-set length ξ_s in determining the relaxation time τ have been reported in Reference 93. In the left panel of **Figure 12**, the relaxation time is plotted as a function of the (scaled) point-to-set length scale for three different glass forming models and on the right panel, a similar plot is shown for the length scale obtained from the minimum eigenvalue scaling. The apparently universal behavior shown in these plots suggests a universal dependence of the growing α-relaxation time on a growing static length scale. There is some numerical evidence (96) that suggests that the point-to-set length scale is the same as that obtained from the minimum eigenvalue of the Hessian matrix.

Thus, available numerical data suggest the rather counter-intuitive conclusion that the growth of the α-relaxation time in simple glass-forming liquids is governed primarily by the growth of a static length scale rather than that of the dynamic length scale of DH. One should, however, exercise caution in drawing this conclusion because the scaling arguments used to derive this conclusion are expected to work well only when the relevant length scales are substantially larger than microscopic length scales (e.g., the average interparticle distance in a liquid), whereas the values of the static length scales obtained in all existing studies are of the order of a few interparticle

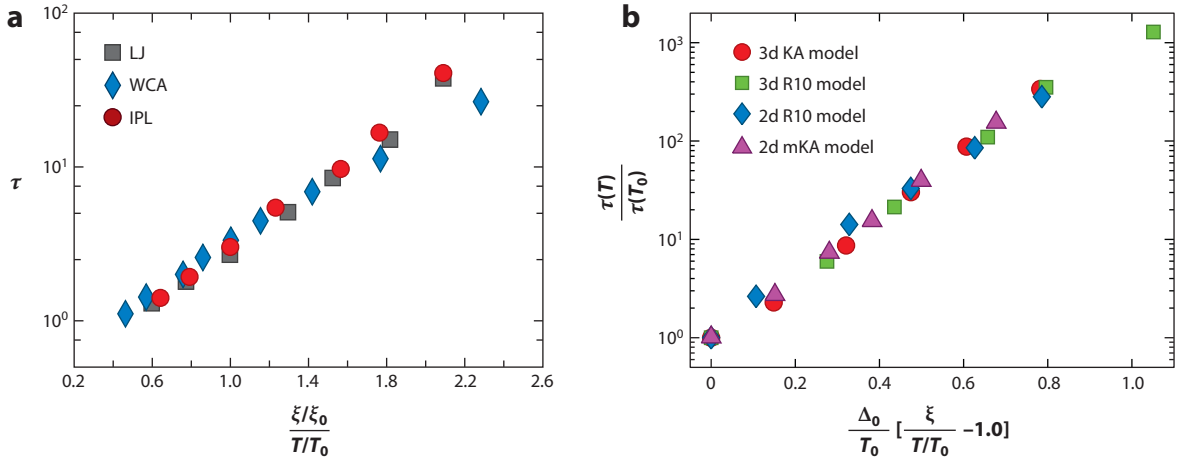

Figure 12

(*a*) The relation between the point-to-set static length scale and the relaxation time for different model systems. Adapted from Reference 93. Abbreviations: IPL, inverse power law; LJ, binary Lennard-Jones; WCA, Weeks-Chandler-Andersen. (*b*) A similar plot for the static length scale obtained from the finite-size scaling of the minimum eigenvalue. Adapted from Reference 105. Here, KA denotes the Kob-Andersen model, R10 denotes a model with $1/r^{10}$ interaction, and mKA denotes a modified Kob-Andersen model. Both plots show similar universal behavior.

spacings. The conclusion about the lack of a causal connection between τ and the dynamic length scale ξ_d seems to be more robust because the values of ξ_d in the temperature range accessible in simulations can be substantially larger than the interparticle spacing.

We close this section with a discussion of what information can be obtained about the values of the RFOT exponents θ and ψ (see Equations 12 and 14) from available numerical data. Because the static length scale ξ_s grows only by a factor of $\sim$2 in the temperature range considered in these studies, it is not possible to extract any information about the exponent θ from the dependence of ξ_s on s_c. The apparently linear behavior seen in the plots in **Figure 12** suggests that the exponent ψ is close to unity. A similar conclusion has also been obtained in References 106 and 107. The validity of the Adam-Gibbs relation in three and four (10) dimensions suggests that $\psi/(d-\theta) = 1$. If $\psi = 1$, then this relation predicts that $\theta = d - 1$. However, if the spatial dimension d is equal to 3 or 4, this violates an inequality, $\psi \geq \theta$, suggested by Fisher & Huse (108) many years ago. It has been argued that this inequality may not be valid for systems with extensive configurational entropy (106). The originally proposed values $\theta = \psi = d/2$ are consistent with the validity of the Adam-Gibbs relation, but there is no clear numerical evidence for these values.

5. CONCLUSIONS AND DISCUSSION

The survey of results given above indicates that although substantial progress has been made in recent years to understand the role of length scales in glass-forming liquids, many questions still remain unanswered. The existence of a growing dynamical length scale, ξ_d, associated with DH is now well established, and its temperature dependence in the range between the onset temperature T_{onset} [the temperature below which nontrivial features such as nonexponential temporal decay of density correlations and super-Arrhenius growth of relaxation times are found in the dynamics (109)] and the critical temperature T_c of MCT has been documented in several studies. There is, however, some uncertainty about the temperature dependence of this length scale below T_c. It is also clear that there is a growing static length scale ξ_s obtained from the point-to-set construction, and there are indications that some of the other static length scales proposed in the literature are in fact the same as this one. This length scale is smaller than ξ_d in the temperature range $T_c < T < T_{\text{onset}}$, and its growth with decreasing temperature is slower than that of ξ_d. There is increasing evidence that suggests that ξ_d and ξ_s are two independent length scales, and the growth of the α-relaxation time τ is governed by ξ_s in the temperature range between T_{onset} and T_c.

An important question in this context is whether this behavior is universal. There are, undoubtedly, many liquids in which local crystalline order plays an important role in determining their static and dynamic behavior at low temperatures. We do not consider such liquids to be generic glass formers. The question we address here is whether the order-agnostic measures of spatial correlations (static or dynamic) considered above exhibit universal behavior in generic glass-forming liquids that do not show pronounced local crystalline order. The degree of universality found in critical phenomena should not be expected here because the very nature of the problem (the fact that the behavior of the liquid near the temperature at which a true phase transition is expected cannot be studied in experiments) implies that a large correlation length, which leads to universality in critical phenomena, cannot be realized in glass-forming liquids. The necessity of using computer simulations to determine the relevant length scales further reduces the temperature range and hence the range of length scales accessible in studies of glass-forming liquids. Also, the presence of two apparently independent length scales (ξ_d and ξ_s) with comparable magnitudes in the accessible temperature range makes it difficult to analyze the role of these length scales in determining various physical properties of the liquid. Given these

difficulties, the degree of universality found in the results shown in **Figures 7*b*** and **12**, in which a simple scaling procedure is used to compare the results for several model liquids, is encouraging. Clearly, extension of these results to temperatures lower than T_c (which will require the development of efficient algorithms to equilibrate liquids at lower temperatures) would be most desirable.

The available results for ξ_d and ξ_s do not provide an answer to the often asked question of whether there is a true glass transition. Although this is an interesting question, an answer is not necessary for understanding the experimentally observed phenomenology of glass-forming liquids. The results summarized above indicate that a growth of the relevant length scale (ξ_s in most studies) by a factor of ~10 would be adequate for explaining the experimentally observed increase of the viscosity and the relaxation time. It is not necessary to know whether the length scale would actually diverge at a putative phase transition at a lower temperature. For the same reason, discussions of the values of the exponents that characterize the growth of the length scales are not particularly meaningful. The range of length scales accessible in simulations and possible experiments is too small for an accurate determination of the exponents.

We close with a discussion of some of the questions raised by the results summarized above and suggestions for future work that would address some of these questions:

1. The growth of the α-relaxation time in the temperature range $T_c < T < T_{\rm onset}$ appears to be governed primarily by the growth of the static length scale ξ_s, which, in turn, is determined by the properties of the underlying (free) energy landscape (the configurational entropy or the lowest eigenvalue of the dynamical matrix). This goes against the expectation, based on analogies with spin-glass models, that the effects of activated processes involving the properties of the energy landscape become important only at temperatures close to and below T_c. This problem would not arise if the theoretically calculated temperature of dynamic arrest in MCT (not the T_c obtained from a power-law fit of the high-temperature data for τ) were taken to be the temperature at which a crossover to activated dynamics should occur, because this temperature is close to $T_{\rm onset}$ (110). This choice, however, would mean that the predictions of MCT are not observed in any temperature range because the dynamics for $T > T_{\rm onset}$ are trivial. Clearly, a detailed investigation of how the predictions of MCT are affected by activated processes would be most interesting in sorting out these issues (111).
2. Most of the existing results for the length scale ξ_d of DH have been obtained from studies of multipoint correlations and susceptibilities. However, the clusters of fast and slow particles, discussed in Section 2, provide a more physical picture of DH, and it would be interesting to extract characteristic length and timescales of DH from the structure and dynamics of these clusters. Some progress in this direction has been made recently in Reference 27, where it was shown that clusters of slow particles are associated with structural relaxation at timescale τ, whereas clusters of fast particles are closely related to particle diffusion with a timescale proportional to t^*, the time at which the non-Gaussian parameter $\alpha_2(t)$ peaks. It would be interesting to try to extract the length scales associated with these two timescales from the geometry of the clusters. Although the string length identified in Reference 27 and previous works is immune to the arbitrariness of definition (inasmuch as it is identified as a small subset of mobile particles that move cooperatively), absolute sizes and statistics of mobile and immobile particle clusters are subject to ambiguities arising from their definitions, which involve well-motivated but arbitrary cutoffs. It would also be useful to identify and study the restructuring events that break up these clusters.

3. There exist intriguing connections between the length scales discussed above and the properties of the low-frequency eigenvalues and eigenvectors of the Hessian matrix of the inherent structures whose basins are visited by the system during the system's time evolution. The eigenvectors are strongly correlated with the spatial structure of DH (and, hence, to the dynamic length ξ_d), whereas the static length scale ξ_s, which appears to govern the growth of the structural relaxation time τ (which is also the characteristic lifetime of DH), is closely related to the smallest eigenvalue. It would be most interesting to explore this connection further, with the objective of determining these length scales from the properties of the Hessian matrix.
4. Although we have concentrated here on the α-relaxation time τ, there are other characteristic timescales in glassy relaxation. These include t^*, the time at which $\alpha_2(t)$ peaks, and τ_β, the timescale of the short-time β relaxation. These timescales also grow as T is decreased. It would be interesting to find out whether the growth of these timescales is governed by one of the length scales discussed above. Inhomogeneous MCT (40) predicts that the growth of τ_β is governed by the length scale ξ_d of DH. Given that activated processes are expected to be less important in short-time dynamics, this prediction of inhomogeneous MCT is more likely to be satisfied in real liquids. A few investigations of the length scale associated with β relaxation exist in the literature (36, 87), but the results are inconclusive. Further work along this line would be useful.
5. Existing numerical results suggest that the point-to-set length, the mosaic length of RFOT theory, the length obtained from the lowest eigenvalue of the Hessian matrix, and the length that describes the system-size dependence of the configurational entropy are all the same. The length scale obtained from a finite-size scaling analysis of the system-size dependence of the configurational entropy measures the system size below which the total configurational entropy becomes subextensive (the entropy per particle becomes lower than the value for large systems). A naive interpretation of the proposal for extracting a static length scale from the frequency of occurrence of patches of different size suggests that the configurational entropy would become subextensive if the system size were smaller than the patch repetition length. Thus, there are reasons to expect that the static length scale ξ_s is also the patch repetition length. This is encouraging because if this is true, then one does not have to deal with a plethora of static length scales. It is, of course, necessary to check whether this equality of different static length scales continues to remain valid at lower temperatures and for different model systems.

DISCLOSURE STATEMENT

The authors are not aware of any affiliations, memberships, funding, or financial holdings that might be perceived as affecting the objectivity of this review.

LITERATURE CITED

1. Debenedetti P. 1997. *Metastable Liquids*. Princeton, NJ: Princeton Univ. Press
2. Berthier L, Biroli G. 2011. *Rev. Mod. Phys.* 83:587–645
3. Angell CA. 1988. *J. Phys. Chem. Solids* 49:863–71
4. Vogel H. 1921. *Z. Phys.* 22:645–56
5. Fulcher GS. 1925. *J. Am. Ceram. Soc.* 8:339–45
6. Tammann D. 1925. *J. Soc. Glass Technol.* 9:166–84
7. Martinez-Garcia JC, Rzoska SJ, Drozd-Roska A, Martinez-Garcia J. 2013. *Nat. Commun.* 4:1823

8. Kauzmann W. 1948. *Chem. Rev.* 43:219–56
9. Adam G, Gibbs JH. 1965. *J. Chem. Phys.* 43:139–46
10. Sengupta S, Karmakar S, Dasgupta C, Sastry S. 2012. *Phys. Rev. Lett.* 109:095705
11. Hohenberg PC, Halperin BI. 1977. *Rev. Mod. Phys.* 49:435–79
12. Young AP, ed. 1998. *Spin Glasses and Random Fields*. Singapore: World Sci.
13. Montanari A, Semerjian G. 2006. *J. Stat. Phys.* 124:103–89
14. Garrahan JP, Sollich P, Toninelli C. 2011. See Ref. 112, pp. 341–66
15. Keys AS, Hedges LO, Garrahan JP, Glotzer SC, Chandler D. 2011. *Phys. Rev. X* 1:021013
16. Liu AJ, Nagel SR, van Saarloos W, Wyart M. 2011. See Ref. 112, pp. 298–336
17. Barrat J-L, Lemaitre A. 2011. See Ref. 112, pp. 265–93
18. Lubchenko V, Wolynes PG. 2007. *Annu. Rev. Phys. Chem.* 58:235–66
19. Ediger MD. 2000. *Annu. Rev. Phys. Chem.* 51:99–128
20. Cipellitti L, Weeks EW. 2011. See Ref. 112, pp. 110–43
21. Harrowell P. 2011. See Ref. 112, pp. 229–59
22. Chaudhuri P, Berthier L, Kob W. 2007. *Phys. Rev. Lett.* 99:060604
23. Kob W, Donati C, Plimpton SJ, Poole PH, Glotzer SC. 1997. *Phys. Rev. Lett.* 79:2827–30
24. Weeks ER, Crocker JC, Levitt AC, Schofeld A, Weitz DA. 2000. *Science* 287:627–31
25. Donati C, Glotzer SC, Poole PH, Kob W, Plimpton SJ. 1999. *Phys. Rev. E* 60:3107–19
26. Langer JS. 2006. *Phys. Rev. Lett.* 97:115704
27. Starr FW, Douglas JF, Sastry S. 2013. *J. Chem. Phys.* 138:12A541
28. Giovambattista N, Buldyrev SV, Stanley HE, Starr FW. 2005. *Phys. Rev. E* 72:011202
29. Dasgupta C, Indrani AV, Ramaswamy S, Phani MK. 1991. *Europhys. Lett.* 15:307–12
30. Donati C, Franz S, Glotzer SC, Parisi G. 2002. *J. Non-Cryst. Solids* 307–310:215–24
31. Franz S, Parisi G. 2000. *J. Phys. Condens. Matter* 12:6335
32. Lacevic N, Starr FW, Schroder TB, Novikov VN, Glotzer SC. 2002. *Phys. Rev. E* 66:030101
33. Flenner E, Szamel G. 2009. *Phys. Rev. E* 79:051502
34. Dauchot O, Marty G, Biroli G. 2005. *Phys. Rev. Lett.* 95:265701
35. Flenner E, Szamel G. 2010. *Phys. Rev. Lett.* 105:217801
36. Flenner E, Zhang M, Szamel G. 2011. *Phys. Rev. E* 83:051501
37. Kim K, Saito S. 2013. *J Chem. Phys.* 138:12A506
38. Karmakar S, Dasgupta C, Sastry S. 2009. *Proc. Natl. Acad. Sci. USA* 106:3675–79
39. Biroli G, Bouchaud J-P, Miyazaki K, Reichman DR. 2006. *Phys. Rev. Lett.* 97:195701
40. Berthier L, Biroli G, Bouchaud J-P, Kob W, Miyazaki K, Reichman DR. 2007. *J. Chem. Phys.* 126:184503
41. Götze W. 2008. *Complex Dynamics of Glass-Forming Liquids: A Mode-Coupling Theory*. Oxford: Oxford Univ. Press
42. Das SP. 2004. *Rev. Mod. Phys.* 76:785–851
43. Sengupta S, Karmakar S, Dasgupta C, Sastry S. 2013. *J. Chem. Phys.* 138:12A548
44. Chong S-H, Kob W. 2009. *Phys. Rev. Lett.* 102:025702
45. Kirkpatrick TR, Wolynes PG. 1987. *Phys. Rev. B* 36:8552–64
46. Kirkpatrick TR, Wolynes PG. 1987. *Phys. Rev. A* 35:3072–80
47. Kirkpatrick TR, Thirumalai D. 1987. *Phys. Rev. B* 36:5388–97
48. Kirkpatrick TR, Thirumalai D. 1987. *Phys. Rev. A* 37:4439–48
49. Kirkpatrick TR, Thirumalai D. 1987. *Phys. Rev. B* 37:5342–50
50. Kirkpatrick TR, Thirumalai D. 1989. *J. Phys. A* 22:L149
51. Thirumalai D, Kirkpatrick TR. 1988. *Phys. Rev. B* 38:4881–92
52. Kirkpatrick TR, Thirumalai D, Wolynes PG. 1989. *Phys. Rev. A* 40:1045–54
53. Bouchaud J-P, Biroli G. 2004. *J. Chem. Phys.* 121:7347–54
54. Kim K. 2003. *Europhys. Lett.* 61:790–95
55. Kob W, Roldan-Vargas S, Berthier L. 2012. *Nat. Phys.* 8:164–67
56. Berthier L, Kob W. 2012. *Phys. Rev. E* 85:011102
57. Kawasaki T, Araki T, Tanaka H. 2007. *Phys. Rev. Lett.* 99:215701

58. Shintani H, Tanaka H. 2008. *Nat. Mater.* 7:870–77
59. Leocmach M, Tanaka H. 2012. *Nat. Commun.* 3:974
60. Tanaka H. 2012. *Eur. Phys. J. E* 35:113
61. Dzugutov M, Simdyankin SI, Zetterling FHM. 2002. *Phys. Rev. Lett.* 89:195701
62. Coslovich D. 2011. *Phys. Rev. E* 83:051505
63. Pedersen UR, Schroder TB, Dyre JC, Harrowell P. 2010. *Phys. Rev. Lett.* 104:105701
64. Steinhardt PJ, Nelson DR, Ronchetti M. 1983. *Phys. Rev. B* 28:784–805
65. Malins A, Eggers J, Royall CP, Williams SR, Tanaka H. 2013. *J. Chem. Phys.* 138:12A535
66. Bruning R, St-Onge DA, Patterson S, Kob W. 2009. *J. Phys. Condens. Matter* 21:035117
67. Kivelson D, Kivelson SA, Zhao X-L, Nussinov Z, Tarjus G. 1995. *Physica* (*Amst.*) 219A:27–38
68. Tarjus G, Kivelson D. 1995. *J. Chem. Phys.* 103:3071–73
69. Chayes L, Emery VJ, Kivelson SA, Nussinov Z, Tarjus G. 1996. *Physica* (*Amst.*) 225A:129–53
70. Nussinov Z, Rudnick J, Kivelson SA, Chayes L. 1999. *Phys. Rev. Lett.* 83:472–75
71. Tarjus G, Kivelson SA, Nussinov Z, Viot P. 2005. *J. Phys. Condens. Matter* 17:R1143
72. Kurchan J, Levine D. 2009. *J. Phys. A* 44:035001
73. Karmakar S, Lerner E, Procaccia I. 2012. *Physica A* 391:1001
74. Philips WA, ed. 1981. *Amorphous Solids: Low Temperature Properties, Topics in Current Physics*, Vol. 24. Berlin: Springer-Verlag
75. Öttinger HC. 2006. *Phys. Rev. E* 74:011113
76. Del Gado E, Ilg P, Kröger M, Öttinger HC. 2008. *Phys. Rev. Lett.* 101:095501
77. Mosayebi M, Del Gado E, Ilg P, Öttinger HC. 2010. *Phys. Rev. Lett.* 104:205704
78. Berthier L, Biroli G, Bouchaud J-P, Cipelletti L, El Masri D, et al. 2005. *Science* 310:1797–1800
79. Dalle-Ferrier C, Thibierge C, Alba-Simionesco C, Berthier L, Biroli G, et al. 2007. *Phys. Rev. E* 76:041510
80. Hurley MM, Harrowell P. 1995. *Phys. Rev. E* 52:1694–98
81. Yamamoto R, Onuki A. 1997. *J. Phys. Soc. Jpn.* 66:2545–48
82. Poole PH, Donati C, Glotzer SC. 1998. *Physica A* 261:51–59
83. Appignanesi GA, Rodriguez-Fris JA. 2009. *J. Phys. Condens. Matter* 21:203103
84. Berthier L. 2003. *Phys. Rev. Lett.* 91:055701
85. Binder K. 1981. *Z. Phys. B* 43:119–40
86. Kob W, Andersen HC. 1994. *Phys. Rev. Lett.* 73:1376–79
87. Stein RLS, Andersen HC. 2008. *Phys. Rev. Lett.* 101:267802
88. Karmakar S, Dasgupta C, Sastry S. 2010. *Phys. Rev. Lett.* 105:019801
89. Karmakar S, Dasgupta C, Sastry S. 2010. *Phys. Rev. Lett.* 105:015701
90. Flenner E, Szamel G. 2012. *Nat. Phys.* 8:696–97
91. Biroli G, Bouchaud J-P, Cavagna A, Grigera TS, Verrocchio P. 2008. *Nat. Phys.* 4:771–75
92. Grigera TS, Parisi G. 2001. *Phys. Rev. E* 63:45102
93. Hocky GM, Markland ME, Reichman DR. 2012. *Phys. Rev. Lett.* 108:225506
94. Charbonneau B, Charbonneau P, Tarjus G. 2012. *Phys. Rev. Lett.* 108:035701
95. Charbonneau P, Tarjus G. 2012. *Phys. Rev. E* 87:042305
96. Biroli G, Karmakar S, Procaccia I. 2013. *Phys. Rev. Lett.* 111:165701
97. Widmer-Cooper A, Perry H, Harrowell P, Reichman DR. 2008. *Nat. Phys.* 4:711–15
98. Widmer-Cooper A, Perry H, Harrowell P, Reichman DR. 2009. *J. Chem. Phys.* 131:194508
99. Brito C, Wyart M. 2007. *J. Stat. Mech.* 08:L08003
100. Chen K, Ellenbroek WG, Zhang Z, Chen DTN, Yunker PJ, et al. 2010. *Phys. Rev. Lett.* 105:025501
101. Franz S, Montanari A. 2007. *J. Phys. A* 40:F251–57
102. Glotzer SC, Novikov VN, Schröder TB. 2000. *J. Chem. Phys.* 112:509–12
103. Glotzer SC. 2000. *J. Non-Cryst. Solids* 274:342–55
104. Hentschel HGE, Karmakar S, Lerner E, Procaccia I. 2011. *Phys. Rev. E* 83:061101
105. Karmakar S, Procaccia I. 2012. *Phys. Rev. E* 86:061502
106. Cammarota C, Cavagna A, Gradenigo G, Grigera TS, Verrocchio P. 2009. *J. Chem. Phys.* 131:194901
107. Cammarota C, Biroli G, Tarzia M, Tarjus G. 2011. *Phys. Rev. Lett.* 106:155705

108. Fisher DS, Huse DA. 1988. *Phys. Rev. B* 38:373–85
109. Sastry S. 2000. *PhysChemComm* 3:79–83
110. Brumer Y, Reichman DR. 2004. *Phys. Rev. E* 69:041402
111. Bhattacharyya SM, Bagchi B, Wolynes PG. 2008. *Proc. Natl. Acad. Sci. USA* 105:16077–82
112. Berthier L, Biroli G, Bouchaud J-P, Cipelletti L, van Saarloos W, eds. 2011. *Dynamical Heterogeneities in Glasses, Colloids and Granular Media*. New York: Oxford Univ. Press